Classification

BIOLOGICAL SCIENCES: Microbiology

Title

Chaperone mediated coupling of subunit availability to activation of proton motive force-driven flagellar Type III Secretion

Running title

Subunit-coupled activation of flagellar export

Authors

Owain J. Bryant[a], Betty Y-W. Chung[a] and Gillian M. Fraser[a,1]

Affiliations

[a]Department of Pathology, University of Cambridge, Tennis Court Road, Cambridge, CB2 1QP, United Kingdom.

Corresponding author

[1]Gillian M. Fraser

Department of Pathology, University of Cambridge, Tennis Court Road, Cambridge, CB2 1QP, United Kingdom.

Phone: +44 1223 330245

Email: gmf25@cam.ac.uk

Keywords

bacterial flagella biogenesis; Type III Secretion System; proton motive force; protein export

Abstract

Bacterial flagella are assembled from thousands of protein subunits that are unfolded and exported across the cell membrane by a specialized flagellar Type III Secretion System (fT3SS). Export of subunit cargo is fuelled by the proton motive force (pmf), facilitated by an export ATPase that is evolutionarily related to the F1 ATPase. The FliJ stalk component of the ATPase binds the flagellar export gate, enabling it to utilise the pmf electric potential (ΔΨ) to drive efficient export of subunit cargo. What is unclear is how FliJ activation of the export gate is regulated to prevent constitutive proton influx and wasteful dissipation of pmf when no subunit cargo is available. FliJ, in addition to activating the export gate, recruits unladen export chaperones and transfers them to cognate subunit cargo, creating a local cycle of chaperone-subunit binding and release at the fT3SS. To investigate whether chaperones might regulate FliJ activation of the export gate, we isolated chaperone variants that were defective for FliJ binding yet still able to bind cognate subunits and other export components. Disruption of the chaperone-FliJ interaction attenuated motility and cognate subunit export. *In vitro* and *in vivo* competitive binding assays showed that chaperones and the export gate component FlhA compete for binding FliJ. Our data indicate that unladen chaperones, which would be present in the cell when subunit levels are low, sequester FliJ to prevent activation of the export gate. This suggests a mechanism whereby chaperones couple availability of export cargo to utilization of pmf by the fT3SS.

Significance

Type III Secretion Systems (T3SS) are used by bacteria to build flagella, rotary nanomachines for cell motility, and related injectosomes, specialised molecular syringes that deliver bacterial effector proteins into host cells to subvert their function. T3SS activity uses two power sources – the high-energy ATP molecule and the proton motive force (pmf), chemical and electric potential stored in a proton gradient

across the bacterial membrane. Here, we show that use of pmf by the flagellar T3SS is regulated by cytoplasmic chaperones that bind and deliver cargo proteins to the T3SS for export. We demonstrate that when cargo availability is low, the unladen chaperones bind the T3SS to reduce its activity, minimising energy use and preventing wasteful dissipation of the pmf.

Introduction

Bacterial flagella are large macromolecular rotary motors that enable cell motility. In *Salmonella,* the long helical flagellar filament propeller that extends from the cell surface is connected to a flexible hook attached to a basal body spanning the cell envelope. These flagellar substructures are assembled in a strict order, with the basal body being constructed first, followed by the hook and then the filament (1, 2). The filament comprises thousands of copies of the major filament subunit, FliC (flagellin), together with three minor filament-class subunits: eleven copies each of FlgK and FlgL form a junction connecting the semi-rigid filament to the hook, and five FliD subunits assemble at the distal tip of the nascent flagellum to form a cap that facilitates folding and incorporation of flagellin into the growing filament (3).

Export of the filament subunits is facilitated by the cytoplasmic chaperones FlgN, FliT and FliS, which bind the C-terminal domains of their cognate structural subunits (FlgN binds FlgK and FlgL, FliT binds FliD, and FliS binds FliC) (4-6). The chaperones then pilot their cognate subunits to the specialized flagellar Type III secretion system (fT3SS) machinery at the base of each flagellum (7-11). Chaperone-subunit complexes initially dock at the FliI component of the flagellar export ATPase, which is evolutionarily related to the F1-ATPase (12). Chaperoned subunits are then thought to interact with the integral membrane export gate component FlhA, where chaperones are released and the subunit cargo is unfolded for translocation across the inner membrane, *via* the FlhAB-FliPQR export gate, into

85 a narrow central channel in the growing flagellum (9-13). Once released from their
86 cognate subunit cargo, the unladen chaperones FlgN and FliT - but not the flagellin
87 chaperone, FliS - are recruited by the FliJ stalk component of the ATPase, which
88 transfers them to newly synthesised cognate cargo to create a local cycle of
89 chaperone-subunit binding at the membrane fT3SS (8). This is thought to promote
90 export of the minor filament subunits that form the hook-filament junction and the
91 filament cap, which are required for initiation of filament assembly (14).
92
93 Export of flagellar subunit cargo across the membrane is powered by the pmf and the
94 flagellar ATPase complex(15, 16). Specifically, the ATPase is thought to facilitate
95 unfolding of subunit cargo (17). In addition, analogous to F- and V-type ATPases,
96 ATP hydrolysis is proposed to drive rotation of the ATPase stalk, FliJ, which interacts
97 with the nonameric export gate component, FlhA, converting the gate into a highly
98 efficient proton-protein antiporter that utilises the ΔΨ electric component of the pmf
99 (18). What is unclear is how FliJ activation of the export gate is regulated in the
100 absence of subunit cargo to prevent constitutive proton influx and wasteful
101 dissipation of the pmf. One way in which export gate activation could be regulated is
102 by sequestration of FliJ by other binding partners, specifically the export chaperones
103 FlgN and FliT. A role for chaperones in the regulation of T3SS activity is supported
104 by the finding that the *Psuedomonas* virulence T3SS chaperone PcrG binds the FliJ
105 homologue, PscO, and that loss of this interaction results in upregulation of effector
106 secretion and renders the T3SS more resistant to pmf collapse (19). These
107 observations suggest that the chaperone-FliJ interaction is central to the regulation of
108 T3SS activity, however, the mechanistic basis of this regulation remains obscure.
109
110 Here, we identify point mutant variants of the chaperones FlgN and FliT that are
111 specifically defective for binding to the FliJ ATPase stalk yet retain the ability to bind
112 cognate subunits and the FlhA component of the fT3SS export gate. We show, *in*

113 *vitro* and *in vivo*, that the FlgN and FliT chaperones compete with FlhA for binding to
114 FliJ, and that chaperone sequestration of FliJ blocks the activating interaction
115 between FliJ and the export gate. This suggests a mechanism whereby binding of
116 FliJ by unladen chaperones acts as a signal to the export machinery that subunit
117 cargo is unavailable and, accordingly, export activity is limited to prevent wasteful
118 dissipation of the pmf. This model is supported by ribosome profiling data, which
119 show that the cytoplasmic ratios of cognate subunits to chaperones are low for FlgN
120 and FliT, relative to the ratio of flagellin to its chaperone, FliS, suggesting that levels
121 of unladen FlgN and FliT would be a sensitive proxy measure of intracellular flagellar
122 subunit levels. Our data reveal the mechanistic basis by which chaperones modulate
123 the FliJ-FlhA interaction to regulate energy use by the T3SS in response to subunit
124 availability.
125

126 **Results and Discussion**

127 ***Isolation of chaperone variants that are specifically defective for FliJ binding***

128 To investigate the function of chaperone binding to the ATPase stalk, FliJ, we sought
129 to identify variants of the FlgN and FliT chaperones that did not bind FliJ yet could
130 interact with cognate subunits and the FlhA component of the fT3SS export gate. To
131 do this, we first constructed mutant alleles of *flgN* encoding variants with three-
132 residue deletions in the FlgN α3 helix (residues 70-102), which contains the
133 overlapping binding sites for cognate subunits and FliJ (Fig. 1; *SI Appendix*, Fig. S1)
134 (8). Screening of the FlgN deletion variants using affinity chromatography pull-down
135 assays with GST- FlgK subunit or GST-FliJ identified a single deletion variant,
136 FlgNΔ76-78, that could bind its cognate subunit but not the ATPase stalk (Fig. 1*B*).
137 Protein sequence comparisons revealed FlgN W_{78} to be highly conserved and
138 replacement of this residue with alanine (FlgN-W_{78}A) severely reduced FlgN binding
139 to FliJ but did not affect binding to FlgK subunit (Fig. 1*C*; FlgNΔ90-100, which binds

140 neither cognate subunit nor FliJ, and wildtype FlgN were included as negative and
141 positive controls, respectively) (8). Affinity chromatography pull-down assays
142 confirmed that FlgNΔ76-78 and FlgN-W_{78}A could still bind the cytoplasmic domain of
143 the export gate component FlhA (GST-FlhAc; Fig. 1*C*).
144
145 Having identified residues in the FlgN α3 helix that, when mutated, could decouple
146 chaperone binding of cognate subunits and FliJ, we targeted conserved residues in
147 the equivalent α3 helix of FliT for site directed mutagenesis to alanine (Fig. 1*D*; *SI*
148 *Appendix*, Fig. S1). To facilitate screening for FliJ binding, mutations were introduced
149 into a *fliT* allele encoding a truncated variant, $FliT_{94}$, which lacks the α4 helix and
150 shows enhanced binding to FliJ *in vitro* (20). Affinity chromatography pull-down
151 assays identified five $FliT_{94}$ variants (I_{68}A, L_{72}A, N_{74}A, E_{75}A and L_{78}A) that showed
152 severely reduced binding to GST-FliJ (Fig. 1*E*). Three of these FliJ non-binders -
153 $FliT_{94}$-I_{68}A, $FliT_{94}$-L_{72}A and $FliT_{94}$-N_{74}A - had previously been shown to bind cognate
154 subunit FliD (20). For this reason, and after assessing the expression and stability of
155 these three $FliT_{94}$ variants in *Salmonella* (not shown), we chose to further investigate
156 the function of truncated $FliT_{94}$-L_{72}A and full-length FliT-L_{72}A.
157
158 Binding of FliT-L_{72}A and truncated $FliT_{94}$-L_{72}A to cognate subunit FliD was confirmed
159 using pull-down assays (GST-FliD; *SI Appendix*, Fig. S2). To assess binding to the
160 export gate component FlhA, pull-down assays were carried out using GST-FlhAc
161 that had been incubated with cell lysates containing FliD cognate subunit, which is
162 required for high affinity binding of FliT to FlhA, and either wildtype FliT or full-length
163 FliT-L_{72}A (Fig. 1*F*) (9). The FliT-Y_{106}A variant, which cannot bind FlhA, was included
164 as a negative control (Fig. 1*F*) (11). Data from the pull-down assays indicated that,
165 when bound to cognate subunit FliD, the FliT-L_{72}A variant can bind the FlhA export
166 gate (Fig. 1*F*).
167

168 ***Attenuation of cell motility and cognate subunit export by specific disruption***
169 ***of the chaperone-FliJ interaction***
170 Having identified chaperone variants (FlgNΔ76-78, FlgN-W_{78}A, FliT-L_{72}A) that were
171 specifically defective for FliJ binding yet retained the ability to bind cognate subunits
172 and the fT3SS export gate, we went on to investigate the importance of the
173 chaperone-FliJ interaction for cell motility and subunit export. To enable expression
174 of chaperones at physiological levels, *Salmonella* strains were engineered to carry
175 variant chaperone genes (*flgNΔ76-78*, *flgN-W_{78}A* or *fliT-L_{72}A*) at the natural genetic
176 loci, replacing the wildtype chaperone gene. As negative controls, isogenic
177 *Salmonella* strains in which the chaperone genes were either deleted (Δ*flgN* or Δ*fliT*)
178 or replaced with variant genes encoding export defective chaperones unable to bind
179 either cognate subunit (*flgNΔ90-100*) or the FlhA export gate (*fliT-Y_{106}A*) were also
180 constructed. These strains were assessed for swimming and swarming motility, and
181 for subunit export efficiency relative to wildtype *Salmonella* (Fig. 2).
182
183 Cell populations producing the FlgNΔ76-78 or FlgN-W_{78}A variants, which cannot bind
184 FliJ, showed slightly decreased swimming (70-90%) and swarming (75-90%) motility
185 relative to wildtype *Salmonella*, though their motility was significantly better than that
186 of the *flgN* null strain or cells producing FlgNΔ90-100, which binds neither cognate
187 subunits nor FliJ (Fig. 2*A* and *SI Appendix*, Fig. S2). Secretion of cognate subunit
188 FlgK was also reduced to *c.*50% of wildtype in cells producing either FlgNΔ76-78 or
189 FlgN-W_{78}A, and this was accompanied by a concomitant increase in soluble
190 extracellular FliC (to 140-150% of wildtype), suggesting that assembly of the FlgKL
191 hook-filament junction was impaired, causing inefficient initiation of filament
192 assembly and increased release of unpolymerized FliC into culture supernatants
193 (Fig. 2*B*) (4). As expected, this secretion defect was more severe in the *flgN* null
194 strain and in cells producing FlgNΔ90-100 (Fig. 2*B*).

195

196 Analysis of motility and export phenotypes associated with the FliT chaperone is
197 complicated by the additional function of FliT as a negative regulator of the flagellar
198 master transcriptional activator $FlhD_4C_2$ (21-23). Cells lacking FliT show increased
199 cellular levels of $FlhD_4C_2$, and a concomitant increase in flagellar gene expression
200 that partially alleviates the motility and export defects typically associated with loss of
201 chaperone activity (4). The increased flagellar gene expression in the *fliT* null is
202 reflected by an increase in the cellular level of non-cognate subunit FlgK, which was
203 observed to be 1.4-fold higher than in wildtype (*SI Appendix*, Fig. S3). Similarly, the
204 level of FlgK was 1.4-fold higher in the strain producing the export defective FliT-
205 $Y_{106}A$ (*SI Appendix*, Fig. S3), indicating increased flagellar gene expression that may
206 be caused by sequestration of FliT-$Y_{106}A$ by cytosolic FliD, which would prevent FliT-
207 $Y_{106}A$ binding to FlhC and targeting it for degradation (21-23). However, cellular
208 levels of FlgK in cells producing FliT-$L_{72}A$ were similar to wildtype, suggesting that
209 while FliT-$L_{72}A$ cannot bind FliJ, it retains the ability to bind FlhC and thus regulate
210 flagellar gene expression (*SI Appendix*, Fig. S3).
211

212 Cells producing FliT-$L_{72}A$ displayed wildtype swimming motility but showed a
213 significant defect in population swarming motility relative to wildtype *Salmonella*
214 (*c.*50% of wildtype; Fig. 2A). Moreover, export of cognate subunit FliD was reduced
215 to *c.*50% of wildtype in the FliT-$L_{72}A$ strain. These data suggest that the FliT-FliJ
216 interaction may be required for export of sufficient FliD to promote the increased
217 flagellation required for swarming (24, 25). Cells producing FliT-$Y_{106}A$, which cannot
218 bind FlhA, showed only a slight defect in swimming and swarming motility, while the
219 *fliT* null strain displayed a marginal reduction in swimming to *c.*80% of wildtype, yet
220 an increase in swarming motility (to *c.*110% of wildtype; Fig. 2B). Both the *fliT* null
221 and FliT-$Y_{106}A$ strain showed a significant reduction in FliD export, to 50-60% of
222 wildtype, accompanied by concomitant release of unpolymerized FliC to culture

223 supernatants (to 110% of wildtype; Fig. 2B). The confounding influence of increased
224 flagellar gene expression in these strains, however, makes it difficult to interpret the
225 motility and export phenotypes of the *fliT* null and FliT-Y_{106}A controls, particularly as
226 overexpression of *flhDC* is known to overcome motility defects associated with
227 chaperone loss (26, 27).
228
229 Notwithstanding the difficulties in interpreting the motility and flagellar export
230 phenotypes associated with loss or mutation of *fliT*, the data for FlgNΔ76-78, FlgN-
231 W_{78}A and FliT-L_{72}A indicate that specific loss of chaperone interactions with FliJ,
232 which would break the local chaperone cycle at the fT3SS, result in attenuation of
233 cognate subunit export and cell motility.
234
235 ***Regulation of fT3SS export gate activation by chaperone sequestration of the***
236 ***FliJ ATPase stalk***
237 The identification and characterisation of FlgN and FliT chaperone variants that were
238 specifically unable to bind the FliJ ATPase stalk opened up the possibility of further
239 investigations into whether chaperones might regulate FliJ activation of the fT3SS.
240 To test whether unladen chaperones could dock at FliJ and block FliJ binding to the
241 FlhA export gate, we developed an *in vitro* competition assay in which $FlhA_C$ binding
242 to cobalt bead-immobilized $(His)_6$-FliJ was assessed in the presence of chaperone
243 variants that could interact with FliJ but not $FlhA_C$ ($FliT_{94}$ or FlgN-Y_{122}A) or were
244 defective in binding both FliJ and $FlhA_C$ ($FliT_{94}$-L_{72}A or FlgN-Y_{122}AΔ76-78; Fig. 3*A*).
245 As anticipated, we found that $FlhA_C$ could bind $(His)_6$-FliJ in the presence of
246 chaperone variants that could not bind FliJ (Fig. 3*B*). However, when assays were
247 performed with chaperones that could bind FliJ, the amount of $FlhA_C$ pulled down by
248 FliJ was severely reduced (Fig. 3*B*).
249

250 The *in vitro* competition assay established that the FlgN and FliT chaperones could
251 block FliJ binding to $FlhA_C$, but did not show if activation of the $FlhA_C$ export gate was
252 prevented. To investigate this, an *in vivo* competition assay was developed in which
253 the effect of FlgN-FliJ binding on $FlhA_C$ export activity was tested under conditions
254 where the availability of cognate subunits for FlgN was limited. Specifically, FlgN
255 variants that could bind FliJ but not $FlhA_C$ (FlgN-Y_{122}A) or were defective in binding
256 both FliJ and $FlhA_C$ (FlgN-Y_{122}AΔ76-78) were expressed *in trans* in Δ*flgE* strain, in
257 which flagellar assembly does not progress beyond completion of the rod and the
258 FlgN cognate subunits, FlgK and FlgL, are produced at very low levels (28-30).
259 Under these conditions, we hypothesised that unladen FlgN might disrupt the FliJ-
260 FlhA interaction, preventing activation of the flagellar export gate and inhibiting
261 subunit export. Assays of subunit export in a strain producing FlgN-Y_{122}A, which
262 binds FliJ, resulted in a *c.*75% reduction in FlgD export compared to the strain
263 producing FlgN-Y_{122}AΔ76-78, which cannot bind FliJ (Fig *3C*).
264
265 Taken together, the data from the *in vitro* and *in vivo* competitive binding assays
266 indicate that when cognate subunit availability is low, unladen chaperones block the
267 FliJ-FlhA interaction and prevent FliJ-dependent activation of the flagellar export
268 machinery.
269
270 ***Ribosome profiling reveals low cytoplasmic ratios of minor filament subunits***
271 ***to cognate chaperones, FlgN and FliT***
272 Our accumulating data suggested that, in addition to piloting subunit cargo to the
273 fT3SS, the FlgN and FliT chaperones might be conditional regulators of fT3SS
274 activity that sense and respond to the availability of subunit cargo. To function
275 effectively in the cell, this mechanism - in which unladen chaperones are a proxy
276 measure for subunit availability - would likely require low cytoplasmic ratios of FlgN

277 and FliT to their cognate subunits. To obtain an indication of the cytoplasmic ratios of
278 chaperones and their cognate subunits, we used RNA sequencing (RNA-Seq) and
279 ribosome profiling (Ribo-Seq) (31-34) to assess the *Salmonella* global transcript
280 abundance and translatome, respectively, at late-log growth phase when flagellar
281 gene expression is at its peak. Analysis of these data confirmed that flagellar mRNAs
282 are amongst the most abundant and highly translated in *Salmonella* (Fig. 4*A*). The
283 ribosome profiling data indicated that the ratio of FlgN to its cognate subunits (FlgK
284 and FlgL) was 1:3, and the ratio of FliT to its cognate subunit FliD was 1:4. These
285 chaperone-subunit ratios are low when compared to the 1:43 ratio of FliS chaperone
286 to its cognate subunit FliC (Fig. 4*B*), suggesting that the presence of unbound FlgN
287 and FliT in the cell would provide a sensitive proxy measure of cytoplasmic flagellar
288 subunit levels.
289
290 Taken together with our other findings, the low ratios of FlgN and FliT to their
291 cognate subunits strengthen the view that these unladen chaperones couple subunit
292 availability to pmf-driven export by modulating FliJ-dependent activation of the $FlhA_c$
293 export gate.
294
295 **Conclusions**
296 The synthesis and operation of bacterial flagella is energetically expensive, using an
297 estimated 2% of the cell's energy, and numerous regulatory mechanisms have
298 evolved to increase efficiency of flagella biogenesis and function. Here, we have
299 uncovered the mechanism by which fT3SS chaperones couple the availability of
300 subunit cargo to the energy efficiency of flagellar export. By identifying point mutant
301 variants of the FlgN and FliT chaperones that were specifically unable to bind the FliJ
302 stalk component of the fT3SS ATPase, we showed that the chaperone-FliJ
303 interaction prevents activation of the FlhA export gate component when subunit
304 availability is low, reducing wasteful dissipation of the pmf by the fT3SS machinery.

305

306 Chaperone modulation of fT3SS activity may be important when *Salmonella*
307 encounters environmental conditions in which flagellar gene expression is down-
308 regulated, including during the early stages of host infection (35-38). Our proposed
309 mechanism may also function in related virulence T3SS (vT3SS), as it is compatible
310 with previous observations showing that vT3SS FliJ homologues bind a subset of
311 secretion chaperones, and that loss of this interaction increases effector secretion
312 and renders the T3SS more resistant to pmf collapse (19, 39, 40). Our data suggest
313 a model for a local chaperone cycle at the T3SS machinery that (i) facilitates efficient
314 docking and export of cognate cargo when subunit/effector availability is high, and (ii)
315 prevents constitutive proton influx and wasteful dissipation of the pmf when cargo
316 availability is low (Fig. 5).

317

318 **Materials and Methods**

319 **Bacterial strains, plasmids and growth conditions**

320 Wildtype *Salmonella enterica* serovar Typhimurium (*S. typhimurium*) SJW1103 is
321 motile (41). The Δ*fliT*::K_m^R mutant in which the *fliT* gene was replaced by a
322 kanamycin resistance cassette was constructed using the λ Red recombinase
323 system (42). Strains containing chromosomally encoded FliT or FlgN variants were
324 constructed by *aph*-I-SceI Kanamycin resistance cassette replacement using
325 pWRG730 (42). Bacteria were cultured at 30–37°C in Luria-Bertani (LB) broth
326 containing, where appropriate, ampicillin (100 mg/ml) or chloramphenicol (20 mg/ml)
327 and collected by centrifugation (6,000*g* for 10 min). Recombinant proteins were
328 expressed in *Salmonella* from the isopropyl β-D-thiogalactoside-inducible (IPTG)-
329 inducible plasmid pTrc99a (43).

330

331 Recombinant proteins for purification were expressed in *E.coli* C41 (44) from (IPTG)-
332 inducible pACT7 (45) or pGEX-4T3 (46). To construct recombinant plasmids

333 encoding wildtype or derivative genes, *Salmonella* genes were amplified from
334 chromosomal DNA by PCR or overlap-extension PCR using Q5 High-Fidelity DNA
335 polymerase. PCR products were inserted BamHI/XhoI into pGEX-4T3 or NdeI/BamHI
336 into pACT7 and pTrc99a. Inserts were verified by DNA sequencing (Department of
337 Biochemistry, University of Cambridge). A full list and description of strains and
338 plasmids used in this study can be found in *SI Appendix*, Tables S1 and S2.
339
340 **Affinity chromatography co-purification assays.**
341 Co-purification of proteins expressed in *E.coli* C41 was performed with glutathione-
342 sepharose 4B. Cells were resuspended in buffer A (50 mM sodium phosphate pH7.4,
343 150 mM NaCl, 1mM β–mercaptoethanol) and mechanically lysed with a Constant
344 Systems cell disruptor at 30,000 kPa. Cleared lysates containing GST-tagged
345 proteins were incubated with affinity resin for 1 hour. After extensive washing with
346 buffer A, cell lysates containing overexpressed untagged prey proteins were then
347 incubated with the resin pre-bound GST-bait. Resins were washed extensively with
348 buffer A and proteins eluted by boiling in SDS-PAGE loading buffer. Proteins were
349 separated by SDS-PAGE and immunoblotted.
350
351 **Flagellar subunit export assay**
352 *Salmonella* strains were cultured at 37 °C in LB broth containing ampicillin and 100
353 μM IPTG to mid-log phase (OD_{600nm} 0.6-0.8). Cells were centrifuged (6000*g*, 5 min),
354 resuspended in fresh media and grown for a further 60 min at 37 °C. Cells were
355 pelleted by centrifugation (16,000*g*, 5 min) and the supernatant passed through a 0.2
356 μm nitrocellulose filter. Supernatant proteins were precipitated with 10%
357 trichloroacetic acid (TCA) and 1% Triton-X100 on ice for 1 hour, pelleted by
358 centrifugation (16,000*g*, 10 min), washed with ice-cold acetone and resuspended in
359 SDS-PAGE loading buffer (volumes calibrated according to cell densities). Fractions
360 were analysed by immunoblotting.

361 **Motility assays**

362 For swimming motility, *Salmonella* strains were grown in LB broth to A600nm 1. Two
363 microliters of culture were inoculated into soft tryptone agar (0.25% agar, 10 g/L
364 tryptone, 5g/L NaCl). Plates were incubated at 37 °C for between 4 and 6 hours. For
365 swarming motility, one microliter of overnight cultures grown in LB broth was
366 inoculated onto dried tryptone agar plates (0.6% agar, 10g/L tryptone, 5g/L NaCl)
367 supplemented with 0.3% glucose and incubated at 30 °C for 16 hours.

368

369 **Chaperone-FliJ *in vitro* competition assay**

370 Recombinant proteins were expressed in *E.coli* C41 and cells were mechanically
371 lysed as described for the co-purification assays. Cleared lysates containing His-
372 tagged FliJ were incubated with cobalt affinity resin for 1 hour. After extensive
373 washing, cell lysates containing overexpressed untagged $FlhA_C$ was added to each
374 resin fraction and an equal volume of wildtype FliT94, FliT94 L72A, wildtype FlgN or
375 FlgN W78A was added. Proteins were incubated for 1 hour, the resin was washed
376 extensively with buffer A and proteins were eluted by boiling in SDS-PAGE loading
377 buffer. Proteins were separated by SDS-PAGE and immunoblotted.

378

379 **FlgN-FliJ *in vivo* competition assay**

380 *Salmonella flgE* null strains carrying either pTrc99a encoding *flgN*-$Y_{122}A\Delta$76-78 or
381 *flgN*-$Y_{122}A$ were grown in LB broth containing ampicillin and inducing agent (50 μM
382 IPTG) to A600 1.0. Cells were centrifuged (6000*g*, 5 min) and resuspended in fresh
383 media and grown for a further 60 min at 37°C. Cells were pelleted by centrifugation
384 (16,000*g*, 5 min) and the supernatant passed through a 0.22 μm nitrocellulose filter
385 (Sartorius). Proteins were precipitated with 10% trichloroacetic acid (TCA) and 1%
386 Triton- X100 on ice for 1 hour, pelleted by centrifugation (16,000*g*, 10 min, 4°C),
387 washed with ice-cold acetone and resuspended in SDS-PAGE loading buffer

388 (volumes calibrated according to cell densities). Fractions were analysed by
389 immunoblotting.
390
391 **Ribosome profiling and RNA-Seq**
392 Libraries were prepared essentially as described previously (47, 48) with the
393 following modifications: Cells were grown in LB at 37°C with 180 RPM shaking to
394 A600 1.0. Chloramphenicol was added to the culture to a final concentration of 1500
395 μg/ml, followed by rapid cooling of the culture and harvesting of cells by
396 centrifugation (6,000 g, 1 min, 4°C). The cell pellet was quickly resuspended in 1 ml
397 ice cold bacterial profiling buffer (20 mM Tris-Cl pH 7.5, 140 mM KCl, 5 mM $MgCl_2$,
398 1500 μg/ml chloramphenicol, 0.5 mM dithiothreitol (DTT), 0.5% NP40, 1% Triton X-
399 100, 2.5% Sucrose) and flash-frozen for cryo-grinding in liquid nitrogen. The frozen
400 powder was thawed and clarified by centrifugation (13,000 g, 2 mins, 4°C) followed
401 by adjustment of $A_{254\ nm}$10. Lysates were either snap frozen in liquid nitrogen for
402 storage at -80°C or nuclease treated with RNase 1 (700U, Ambion) followed by
403 ribosomal RNA depletion using a bacterial ribozero kit (Illumina) prior to library
404 preparation for ribosome profiling. For parallel RNA-Seq, total RNA was extracted
405 from corresponding lysates followed ribosomal RNA depletion using the bacterial
406 ribozero kit (Illumina) prior to library preparation. For Ribosome profiling, rRNA was
407 further depleted with duplex-specific nuclease as described previously (47).
408 Ribosome profiling and RNA-Seq libraries were pooled and sequenced using the
409 NextSeq® 500/550 platform and data were trimmed and mapped to the
410 transcriptome assembly of *Salmonella enterica* subsp. *enterica* serovar Typhimurium
411 strain ST4/74 (GenBank accession CP002487.1). Paired ribosome profiling and
412 RNA-Seq analysis was performed with riboSeqR as previously described (48, 49).
413
414

415 **Acknowledgements**

416 We thank Colin Hughes and Lewis Evans for useful discussions, and Sangita Ahmed
417 for technical assistance. This work was funded by grants from the Biotechnology and
418 Biological Sciences Research Council (BB/M007197/1) to G.M.F, Medical Research
419 Council [MR/R021821/1] to B.Y-W.C., and a University of Cambridge John Lucas
420 Walker Studentship to O.J.B.

421

422 **Footnotes**

423 The authors declare no conflict of interest.

424

425 **Author contributions**

426 O.J.B, B.Y-W.C. and G.M.F. designed the research; O.J.B performed the research;
427 O.J.B, B.Y-W.C. and G.M.F. analyzed the data and wrote the paper.

428

429 **References**

430 1. L. D. B. Evans, C. Hughes, G. M. Fraser, Building a flagellum outside the
431 bacterial cell. *Trends. Microbiol*. **22**, 566-572 (2014)

432 2. L. D. B. Evans, C. Hughes, G. M. Fraser. Building a flagellum in biological
433 outer space. *Microb. Cell* **1**, 64-66 (2014)

434 3. K. Yonekura, S. Maki, D. G. Morgan, D. J. DeRosier, F. Vonderviszt *et al.* The
435 bacterial flagellar cap as the rotary promoter of flagellin self-assembly.
436 *Science* **290** (2000)

437 4. J. C. Bennett, J. Thomas, G. M. Fraser, C. Hughes, Substrate complexes and
438 domain organization of the *Salmonella* flagellar export chaperones FlgN and
439 FliT. *Mol. Microbiol.* **39**, 781–791 (2001).

440 5. G. M. Fraser, J. C. Bennett, C. Hughes, Substrate-specific binding of hook-
441 associated proteins by FlgN and FliT, putative chaperones for flagellum
442 assembly. *Mol. Microbiol.* **32**, 569–580 (1999).

443 6. F. Auvray, J. Thomas, G. M. Fraser, C. Hughes, Flagellin polymerisation
444 control by a cytosolic export chaperone. *J. Mol. Biol.* **308**, 221–229 (2001).
445 7. J. Thomas, G. P. Stafford, C. Hughes, Docking of cytosolic chaperone-
446 substrate complexes at the membrane ATPase during flagellar type III protein
447 export. *Proc. Natl. Acad. Sci. U.S.A.* **101**, 3945-3950 (2004).
448 8. L. D. B. Evans, G. P. Stafford, S. Ahmed, G. M. Fraser, C. Hughes, An escort
449 mechanism for cycling of export chaperones during flagellum assembly. *Proc.*
450 *Natl. Acad. Sci. U.S.A.* **103**, 17474–9 (2006).
451 9. G. Bange, N. Kümmerer, C. Engel, G. Bozkurt, K. Wild *et al*. FlhA provides the
452 adaptor for coordinated delivery of late flagella building blocks to the type III
453 secretion system. *Proc. Natl. Acad. Sci. U.S.A.* **107**, 11295–11300 (2010).
454 10. T. Minamino, M. Kinoshita, N. Hara, S. Takeuchi, A. Hida, *et al.* Interaction of
455 a bacterial flagellar chaperone FlgN with FlhA is required for efficient export of
456 its cognate substrates. *Mol. Microbiol.* **83**, 775–788 (2012).
457 11. M. Kinoshita, N. Hara, K. Imada, K. Namba, T. Minamino, Interactions of
458 bacterial flagellar chaperone-substrate complexes with FlhA contribute to co-
459 ordinating assembly of the flagellar filament. *Mol. Microbiol.* **90**, 1249–1261
460 (2013).
461 12. T. Ibuki, K. Imada, T. Minamino, T. Kato, T. Miyata *et al.* Common architecture
462 of the flagellar type III protein export apparatus and F- and V-type ATPases.
463 *Nat. Struct. Mol. Biol.* **18**, 277–282 (2011).
464 13. L. Kuhlen, P. Abrusci, S. Johnson, J. Gault, J. Deme *et al.* Structure of the
465 core of the type iii secretion system export apparatus. *Nat. Struct. Mol. Biol.*
466 **25,** 583-590 (2018).
467 14. M. Homma, K. Kutsukake, T. Iino, S. Yamaguchi, Hook-associated proteins
468 essential for flagellar filament formation in *Salmonella* typhimurium. *J.*
469 *Bacteriol.* **157**, 100-108 (1984).
470 15. T. Minamino, K. Namba, Distinct roles of the FliI ATPase and proton motive

force in bacterial flagellar protein export. *Nature* **451**, 485–488 (2008).

16. K. Paul, M. Erhardt, T. Hirano, D. F. Blair, K. T. Hughes, Energy source of flagellar type III secretion. *Nature* **451**, 489-492 (2008).

17. Y. Akeda, J. E. Galán, Chaperone release and unfolding of substrates in type III secretion. *Nature* **437**, 911–915 (2005).

18. T. Minamino, Y. V. Morimoto, N. Hara, K. Namba, An energy transduction mechanism used in bacterial flagellar type III protein export. *Nat. Commun.* **2**, 475 (2011).

19. P. C. Lee, S. E. Zmina, C. M. Stopford, J. Toska, A. Rietsch, Control of type III secretion activity and substrate specificity by the cytoplasmic regulator PcrG. *Proc. Natl. Acad. Sci. U.S.A.* **111**, E2027–E2036 (2014).

20. K. Imada, T. Minamino, M. Kinoshita, Y. Furukawa, K. Namba, Structural insight into the regulatory mechanisms of interactions of the flagellar type III chaperone FliT with its binding partners. *Proc. Natl. Acad. Sci. U.S.A.* **107**, 8812–8817 (2010).

21. S. Yamamoto, K. Kutsukake, FliT acts as an anti-$FlhD_2C_2$ factor in the transcriptional control of the flagellar regulon in *Salmonella enterica* serovar typhimurium. *J. Bacteriol.* **188**, 6703–6708 (2006).

22. K. Kutsukake, T. Ikebe, S. Yamamoto, Two novel regulatory genes, fliT and fliZ, in the flagellar regulon of *Salmonella*. *Genes. Genet. Syst.* **74**, 287–292 (1999).

23. Y. Sato, A. Takaya, C. Mouslim, K. T. Hughes, T. Yamamoto, FliT selectively enhances proteolysis of FlhC Subunit in $FlhD_4C_2$ complex by an ATP-dependent protease, ClpXP. *J. Biol. Chem.* **289**, 33001–33011 (2014).

24. G. M. Fraser, C. Hughes, Swarming motility. *Curr. Opin. Microbio*l. **2**, 630-635 (1999).

25. D. B. Kearns, A field guide to bacterial swarming motility. *Nat. Rev. Microbiol.* **8**, 634-644 (2010).

499 26. A. Dufour, R. B. Furness, C. Hughes, Novel genes that upregulate the *Proteus*
500 *mirabilis* flhDC master operon controlling flagellar biogenesis and swarming.
501 *Mol. Microbiol.* **29**, 741-751 (1998).
502 27. P. Aldridge, J. Karlinsey, K. T. Hughes, The type III secretion chaperone FlgN
503 regulates flagellar assembly via a negative feedback loop containing its
504 chaperone substrates FlgK and FlgL. *Mol. Microbiol.* **49**, 1333-1345 (2003).
505 28. T. Hirano, T. Minamino, K. Namba, R. M. Macnab, Substrate specificity
506 classes and the recognition signal for *Salmonella* type III flagellar export. *J.*
507 *Bacteriol.* **185**, 2485-2492 (2003).
508 29. K. T. Hughes, K. L. Gillen, M. J. Semon, J. E. Karlinsey, Sensing structural
509 intermediates in bacterial flagellar assembly by export of a negative regulator.
510 *Science* **19**, 1277-1280 (1993).
511 30. K. Kutsukake, Excretion of the anti-sigma factor through a flagellar
512 substructure couples flagellar gene expression with flagellar assembly in
513 *Salmonella* typhimurium. *Mol. Gen. Genet.* **15**, 605-612 (1994).
514 31. R. Lister, R. C. O'Malley, J. Tonti-Filippini, B. D. Gregory, C. C. Berry *et al*.
515 Highly Integrated Single-Base Resolution Maps of the Epigenome in
516 *Arabidopsis*. *Cell* **133**, 523-536 (2008).
517 32. A. Mortazavi, B. A. Williams, K. McCue, L. Schaeffer, B. Wold, Mapping and
518 quantifying mammalian transcriptomes by RNA-Seq. *Nat. Methods* **5**, 621-628
519 (2008).
520 33. U. Nagalakshmi, Z. Wang, K. Waern, C. Shou, D. Raha, *et al*. The
521 transcriptional landscape of the yeast genome defined by RNA sequencing.
522 *Science* 320, 1344-1349 (2008).
523 34. N. T. Ingolia, S. Ghaemmaghami, J. R. Newman, J. S. Weissman, Genome-
524 wide analysis in vivo of translation with nucleotide resolution using ribosome
525 profiling. *Science* **324**, 218-223 (2009).
526 35. I. Spöring, S. Felgner, M. Preuße, D. Eckweiler, M. Rohde *et al.* Regulation of

527 Flagellum Biosynthesis in Response to Cell Envelope Stress in *Salmonella*
528 *enterica* Serovar Typhimurium. *MBio* **9**, e00736-17 (2018).
529 36. P. Adams, R. Fowler, N. Kinsella, G. Howell, M. Farris *et al*. Proteomic
530 detection of PhoPQ- and acid-mediated repression of *Salmonella* motility.
531 *Proteomics* **1**, 597-607 (2005).
532 37. E. A. Miao, J. V. Rajan, *Salmonella* and Caspase-1: A complex interplay of
533 detection and evasion. *Front. Microbiol.* **2**, 85 (2011).
534 38. B. Ilyas, D. T. Mulder, D. J. Little, W. Elhenawy, M. M. Banda *et al.* Regulatory
535 Evolution Drives Evasion of Host Inflammasomes by *Salmonella* Typhimurium.
536 *Cell Rep.* **25**, 825-832 (2018).
537 39. L. D. B. Evans, C. Hughes, Selective binding of virulence type III export
538 chaperones by FliJ escort orthologues InvI and YscO. *FEMS Microbiol.*
539 *Lett*. **293**, 292-297 (2009)
540 40. Y. Cherradi, A. Hachani, A. Allaoui, Spa13 of *Shigella flexneri* has a dual role:
541 Chaperone escort and export gate-activator switch of the type III secretion
542 system. Microbiology. **160**, 130–141 (2014).
543 41. S. Yamaguchi, H. Fujita, T. Taira, K. Kutsukake, M. Homma, *et al*. Genetic
544 analysis of three additional fla genes in *Salmonella* typhimurium. *J. Gen.*
545 *Microbiol.* **130**, 3339-3342 (1984).
546 42. S. Hoffmann, C. Schmidt, S. Walter, J. K. Bender, R. G. Gerlach, Scarless
547 deletion of up to seven methylaccepting chemotaxis genes with an optimized
548 method highlights key function of CheM in *Salmonella* Typhimurium. *PLoS*
549 *One* **12**, e0172630. (2017).
550 43. E. Amann, B. Ochs, K. J. Abel, Tightly regulated tac promoter vectors useful
551 for the expression of unfused and fused proteins in *Escherichia coli*. *Gene* **69**,
552 301-315 (1988).
553 44. B. Miroux, J. E Walker, Over-production of proteins in *Escherichia coli*: Mutant
554 hosts that allow synthesis of some membrane proteins and globular proteins at

555 high levels. *J. Mol. Biol.* **260**, 289-298 (1996).
556 45. T. Thanabalu, E. Koronakis, C. Hughes, V. Koronakis, Substrate-induced
557 assembly of a contiguous channel for protein export from *E.coli*: reversible
558 bridging of an inner-membrane translocase to an outer membrane exit pore.
559 *EMBO J.* **17**, 6487-6496 (1998).
560 46. W. G. Kaelin, W. Krek, W. R. Sellers, J. A. DeCaprio, F. Ajchenbaum, *et al.*
561 Expression cloning of a cDNA encoding a retinoblastoma-binding protein with
562 E2F-like properties. *Cell* **70**, 351-364 (1992).
563 47. B. Y. W. Chung, M. J. Deery, A. J. Groen, J. Howard, D. C. Baulcombe,
564 Endogenous miRNA in the green alga *Chlamydomonas* regulates gene
565 expression through CDS-targeting. *Nat. Plants* **3**, 787-794 (2017).
566 48. B. Y. W. Chung, T. J. Hardcastle, J. D. Jones, N. Irigoyen, A. E. Firth *et al.*
567 The use of duplex-specific nuclease in ribosome profiling and a user-friendly
568 software package for Ribo-seq data analysis. *RNA* **21**, 1731-1745 (2015).
569 49. T. J. Hardcastle, Data from “Analysis of sequencing data from ribosome
570 profiling experiments.” Bioconductor. Available at
571 doi:10.18129/B9.bioc.riboSeqR.
572
573

574 **Figure Legends**

575 **Figure 1 Identification of chaperone variants defective for FliJ binding**

576 **A.** Atomic resolution structure of the 140-residue *Salmonella* FlgN (PDB: 5B3D)
577 indicating the region (residues 70-102; red) in which three-residue scanning deletions
578 were introduced.

579

580 **B.** Affinity chromatography of glutathione sepharose-bound GST-FliJ or GST-FlgK
581 incubated with cell lysates containing wildtype FlgN or its three-amino acid deletion
582 variants. After washing, proteins were eluted in SDS-loading buffer, separated by
583 SDS(15%)-PAGE and stained with Coomassie Brilliant Blue. Apparent molecular
584 weights are in kilodaltons (kDa).

585

586 **C.** Affinity chromatography of glutathione sepharose-bound GST-FliJ, GST-FlgK or
587 GST-FlhAc incubated with cell lysates containing wildtype FlgN or its derivative
588 variants FlgNΔ76-78, FlgN-W78A or FlgNΔ90-100. After washing, proteins were
589 eluted in SDS-loading buffer, separated by SDS(15%)-PAGE and stained with
590 Coomassie Brilliant Blue. Apparent molecular weights are in kilodaltons (kDa).

591

592 **D.** Atomic resolution structure of the 122-residue *Salmonella* FliT (PDB: 3A7M)
593 indicating the position of conserved residues (red) within the region essential for FliJ
594 binding. *In vitro* binding to FliJ is enhanced by truncating FliT at residue 94 (dashed
595 red line).

596

597 **E.** Affinity chromatography of glutathione sepharose-bound GST-FliJ with cell lysates
598 containing FliT94 or its point mutant variants. After washing, proteins were eluted in
599 SDS-loading buffer, separated by SDS(15%)-PAGE and stained with Coomassie
600 Brilliant Blue. Apparent molecular weights are in kilodaltons (kDa).

601

602 **F.** Affinity chromatography of glutathione sepharose-bound GST-FlhAc incubated
603 with cell lysates containing FliD and wildtype FliT or its point mutant variants FliT-
604 L72A or FliT-Y106A. After washing, proteins were eluted in SDS-loading buffer,
605 separated by SDS(15%)-PAGE and stained with Coomassie Brilliant Blue (top panel)
606 or were analysed by immunoblotting with anti-FliT or anti-FliD polyclonal antisera
607 (middle and bottom panels). Apparent molecular weights are in kilodaltons (kDa).
608
609 **Figure 2 FliJ binding to FlgN and FliT is required for efficient cell motility and**
610 **subunit export**
611 **A.** Swimming (top panel; 0.25% soft tryptone agar) and swarming (bottom panels;
612 0.6% agar-tryptone with 0.5% glucose) motility of recombinant *Salmonella* strains
613 producing chromosomally-encoded FlgN variants (W78A, Δ76-78, or Δ90-100), the
614 SJW1103 wildtype, and the *Salmonella flgN* null strain (Δ*flgN*).
615
616 **B.** Whole cell (cell) and supernatant (secreted) proteins from late exponential-phase
617 cultures of *Salmonella* strains producing chromosomally-encoded FlgN variants
618 (W78A, Δ76-78, or Δ90-100), the SJW1103 wildtype, and the *Salmonella flgN* null
619 strain (Δ*flgN*) were separated by SDS (15%)-PAGE and analysed by immunoblotting
620 with anti-FliC, anti-FlgK or anti-FlgN polyclonal antisera. Apparent molecular weights
621 are in kilodaltons (kDa).
622
623 **C.** Swimming (top panel; 0.25% soft tryptone agar) and swarming (bottom panels;
624 0.6% agar-tryptone with 0.5% glucose) motility of recombinant *Salmonella* strains
625 producing chromosomally-encoded FliT variants (L72A and Y106A), the SJW1103
626 wildtype, and the *Salmonella fliT* null strain (Δ*fliT*).
627
628 **D.** Whole cell (cell) and supernatant (secreted) proteins from late exponential-phase
629 cultures of *Salmonella* strains producing chromosomally-encoded FliT variants (L72A

630 and Y106A), the SJW1103 wildtype, and the *Salmonella fliT* null strain (Δ*fliT*) were
631 separated by SDS (15%)-PAGE and analysed by immunoblotting with anti-FliC, anti-
632 FliD or anti-FliT polyclonal antisera. Apparent molecular weights are in kilodaltons
633 (kDa).
634
635 **Figure 3 FlgN and FliT chaperones compete with $FlhA_C$ for binding to FliJ**
636 **A.** *In vitro* competition assay to assess $FlhA_C$ binding to cobalt (Co^{2+}) bead-
637 immobilized $(His)_6$-FliJ in the presence of the FlgN or FliT chaperones, or chaperone
638 variants that cannot bind FliJ (FliJ non-binder).
639
640 **B.** Cell lysates of *E.coli* C41 expressing FliT94, which cannot bind $FlhA_C$ (-), or its
641 L72A variant, which cannot bind $FlhA_C$ or FliJ (left-hand panels), or FlgN Y112A
642 which cannot bind $FlhA_C$ (-) or its Δ76-78 variant, which cannot bind $FlhA_C$ or FliJ
643 (right-hand panels) were mixed with *E.coli* C41 lysates containing FlhAc (load) and
644 incubated with cobalt bead-immobilized $(His)_6$-FliJ (bound). After washing, proteins
645 were eluted from the cobalt beads in SDS-loading buffer, separated by SDS(15%)-
646 PAGE and analysed by immunoblotting with anti-FlhA, anti-FliT, anti-FlgN or anti-FliJ
647 polyclonal antisera. Apparent molecular weights are in kilodaltons (kDa).
648
649 **C.** *In vivo* competition assay to assess the effect of chaperone-FliJ binding on $FlhA_C$
650 export activity. Export of the unchaperoned FlgD subunit was assessed in a *flgE* null
651 strain. Whole cell (cell) and supernatant (secreted) proteins from late exponential-
652 phase cultures of *Salmonella* Δ*flgE* strains producing pTrc99a-encoded FlgN Y122A
653 (-) or FlgN Y122A, Δ76-78 (Δ76-78) were separated by SDS (15%)-PAGE and
654 analysed by immunoblotting with anti-FlgD, anti-FlgN, anti-FliJ and anti-FlhA
655 polyclonal antisera. Apparent molecular weights are in kilodaltons (kDa). Relative
656 amounts of FlgD secreted into culture supernatants were quantified using image
657 Studio Lite software and normalized to FlgD secreted by cells expressing the FlgN

658 Δ76-78 Y122A variant (right-hand bar chart). Export of non-cognate subunit FlgD is
659 attenuated in cells producing FlgN Y122A (-), which binds FliJ but not FlhA, but is
660 significantly higher in cells producing the FlgN variant defective in binding FliJ (FlgN
661 Δ76-78,Y122A).
662
663 **Figure 4 Ribosome profiling reveals cytoplasmic ratios of flagellar subunits to**
664 **their cognate chaperones**
665 **A.** Smoothed scatter plot of total translation (Ribosome profiling, measurement of
666 ribosome occupation) and total mRNA abundance (RNA-Seq), showing flagellar
667 chaperones FlgN, FliT and FliS (blue), their respective cognate subunits (red), and
668 the regression between total translation and mRNA abundance (dotted line).
669
670 **B.** Ratios of the normalised translation to gene length for the coding regions
671 corresponding to chaperones and their cognate subunits (FlgN:FlgK+FlgL; FliT:FliD;
672 FliS:FliC).
673
674 **Figure 5 Chaperone regulation of the fT3SS machinery in response to subunit**
675 **cargo availability**
676 Chaperone-subunit complexes initially dock at the FliI component of the ATPase
677 complex before docking at the cytoplasmic domain of FlhA (left-hand panel).
678 Subunits are subsequently released from their cognate chaperones and translocated
679 into the export channel. Unladen chaperones then bind FliJ from which they are
680 captured by newly synthesized cognate subunits. Under conditions where subunit
681 availability is limited (right-hand panel), unladen FlgN and FliT chaperones remain
682 bound to FliJ, blocking the interaction of FliJ with FlhA and reducing pmf-driven
683 export by the fT3SS machinery.
684
685

686 **Supplementary Figure Legends**

687 **Figure S1.**

688 **A**. Affinity chromatography of glutathione sepharose-bound glutathione-S-transferase
689 (GST) incubated with cell lysates containing FliT94. After washing, proteins were
690 eluted in SDS-loading buffer, separated by SDS(15%)-PAGE and stained with
691 Coomassie Brilliant Blue (top panel). The cell lysate load was analyzed by
692 immunoblotting with polyclonal anti-FliT anti-sera (bottom panel). Apparent
693 molecular weights are in kilodaltons (kDa).

694

695 **B**. Affinity chromatography of glutathione sepharose-bound glutathione-S-transferase
696 (GST) incubated with cell lysates containing FlgN. After washing, proteins were
697 eluted in SDS-loading buffer, separated by SDS(15%)-PAGE and stained with
698 Coomassie Brilliant Blue (top panel). The cell lysate load was analyzed by
699 immunoblotting with polyclonal anti-FlgN anti-sera (bottom panel). Apparent
700 molecular weights are in kilodaltons (kDa).

701

702 **Figure S2.**

703 **A**. Affinity chromatography of glutathione sepharose-bound GST-FlgL (top two
704 panels) or glutathione-S-transferase (GST; bottom panels) incubated with cell lysates
705 containing FlgN or its derivative variants FlgN∆76-78, FlgN-W78A or FlgN∆90-100.
706 After washing, proteins were eluted in SDS-loading buffer, separated by SDS(15%)-
707 PAGE and stained with Coomassie Brilliant Blue to visualise GST-FlgL and GST, or
708 analysed by immunoblotting with polyclonal anti-FlgN anti-sera. The cell lysate load
709 (FlgN load) was also analyzed by immunoblotting with polyclonal anti-FlgN anti-sera.
710 Apparent molecular weights are in kilodaltons (kDa).

711

712 **B**. Affinity chromatography of glutathione sepharose-bound GST-FliJ (top two
713 panels), GST-FliD (middle two panels) or glutathione-S-transferase (GST; bottom

714 panels) with cell lysates containing FliT and its mutant variants. After washing,
715 proteins were eluted in SDS-loading buffer, separated by SDS(15%)-PAGE and
716 stained with Coomassie Brilliant Blue to visualise GST-FliJ, GST-FliD and GST, or
717 analysed by immunoblotting with polyclonal anti-FliT anti-sera. The cell lysate load
718 (FliT load) was also analyzed by immunoblotting with polyclonal anti-FliT anti-sera.
719 Apparent molecular weights are in kilodaltons (kDa).
720
721 **C**. Cell lysates of *E.coli* C41 expressing FliT (top panel) or FliD (bottom panel) used
722 as load fractions in affinity chromatography assays with GST-FlhAc in Figure 1.
723 Proteins were separated by SDS(15%)-PAGE and analysed by immunoblotting with
724 polyclonal anti-FliT anti-sera or polyclonal anti-FliD anti-sera.
725
726 **Figure S3.**
727 **a**. Whole cell and supernatant proteins from late exponential-phase cultures of
728 *Salmonella* strains producing chromosomally-encoded FliT variants (L72A and
729 Y106A), the *Salmonella fliT* null strain (Δ*fliT*), and the SJW1103 wildtype were
730 separated by SDS (15%)-PAGE and analysed by immunoblotting with anti-FlgK
731 polyclonal antisera. Apparent molecular weights are in kilodaltons (kDa).
732
733
734

FIGURE 1

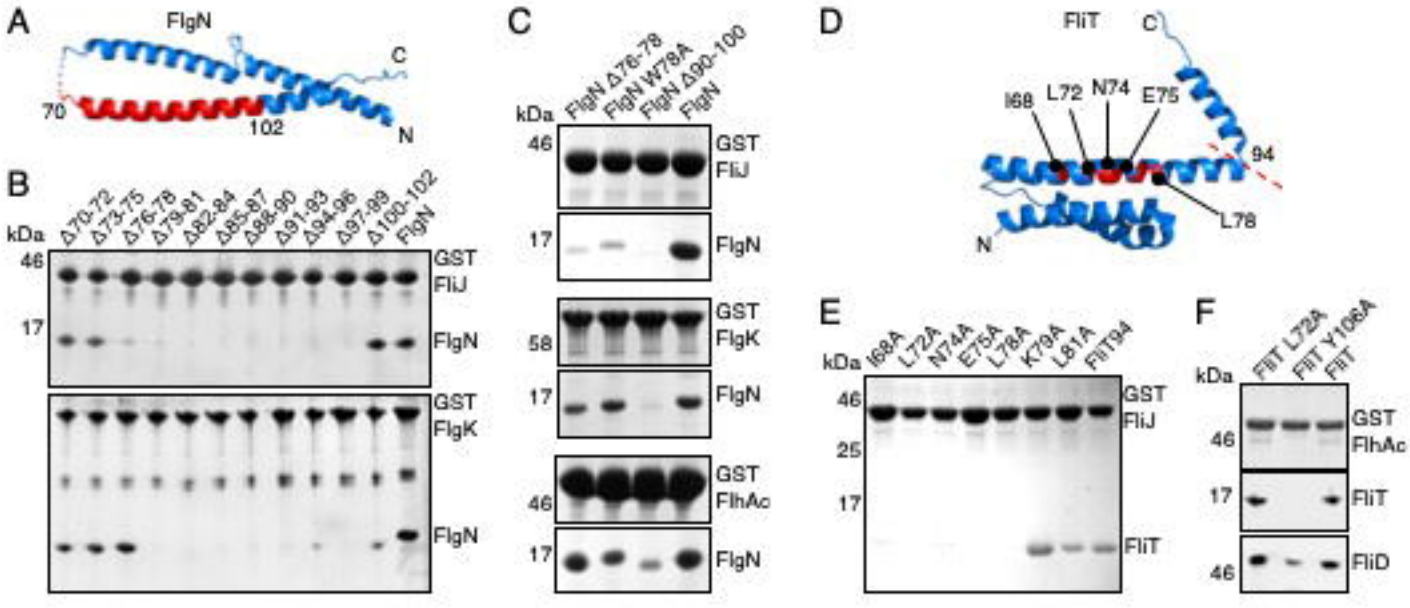
A
FlgN
C
70
102
N
B
kDa
Δ70-72
Δ73-75
Δ76-78
Δ79-81
Δ82-84
Δ85-87
Δ88-90
Δ91-93
Δ94-96
Δ97-99
Δ100-102
FlgN
46
17
GST
FliJ
FlgN
GST
FlgK
FlgN
C
kDa
FlgN Δ76-78
FlgN W78A
FlgN Δ90-100
FlgN
46
GST
FliJ
17
FlgN
58
GST
FlgK
17
FlgN
46
GST
FlhAc
17
FlgN
D
FliT
C
I68
L72
N74
E75
94
L78
N
E
kDa
I68A
L72A
N74A
E75A
L78A
K79A
L81A
FliT94
46
25
17
GST
FliJ
FliT
F
kDa
FliT L72A
FliT Y106A
FliT
46
17
46
GST
FlhAc
FliT
FliD

FIGURE 2

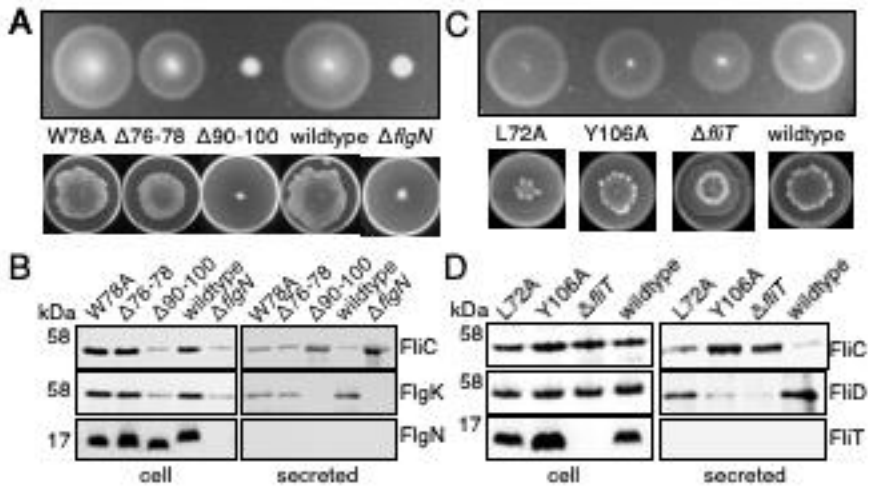
A
W78A Δ76-78 Δ90-100 wildtype ΔflgN
C
L72A Y106A ΔfliT wildtype
B
kDa W78A Δ76-78 Δ90-100 wildtype ΔflgN W78A Δ76-78 Δ90-100 wildtype ΔflgN
58
58
17
FliC
FlgK
FlgN
cell
secreted
D
kDa L72A Y106A ΔfliT wildtype L72A Y106A ΔfliT wildtype
58
58
17
FliC
FliD
FliT
cell
secreted

FIGURE 3

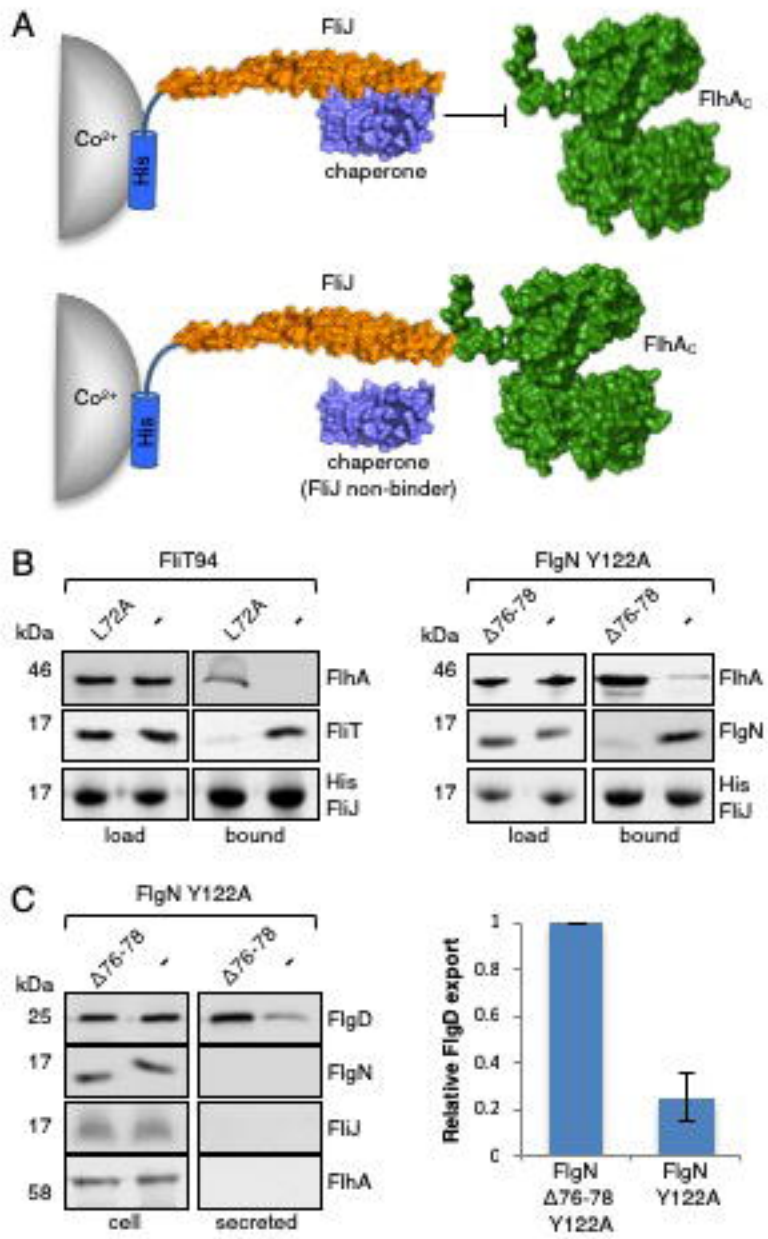
A
FliJ
Co2+
His
chaperone
FlhAC
FliJ
Co2+
His
chaperone
(FliJ non-binder)
FlhAC
B
FliT94
L72A
-
L72A
-
kDa
46
17
17
FlhA
FliT
His
FliJ
load
bound
FlgN Y122A
Δ76-78
-
Δ76-78
-
kDa
46
17
17
FlhA
FlgN
His
FliJ
load
bound
C
FlgN Y122A
Δ76-78
-
Δ76-78
-
kDa
25
17
17
58
FlgD
FlgN
FliJ
FlhA
cell
secreted
Relative FlgD export
1
0.8
0.6
0.4
0.2
0
FlgN Δ76-78 Y122A
FlgN Y122A

FIGURE 4

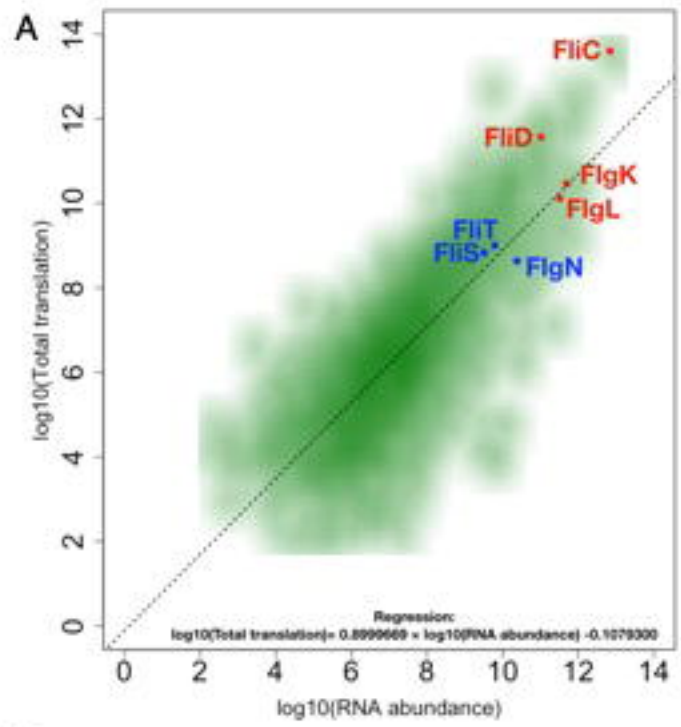
A
FliC
FliD
FlgK
FlgL
FlIT
FliS
FlgN
log10(Total translation)
log10(RNA abundance)
Regression:
log10(Total translation)= 0.8999669 × log10(RNA abundance) -0.1079300
0
2
4
6
8
10
12
14

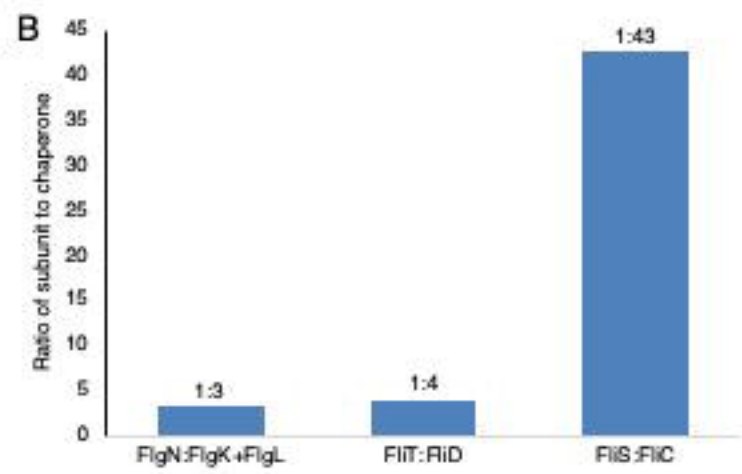
B
Ratio of subunit to chaperone
45
40
35
30
25
20
15
10
5
0
1:3
1:4
1:43
FlgN:FlgK+FlgL
FlIT:FliD
FliS:FliC
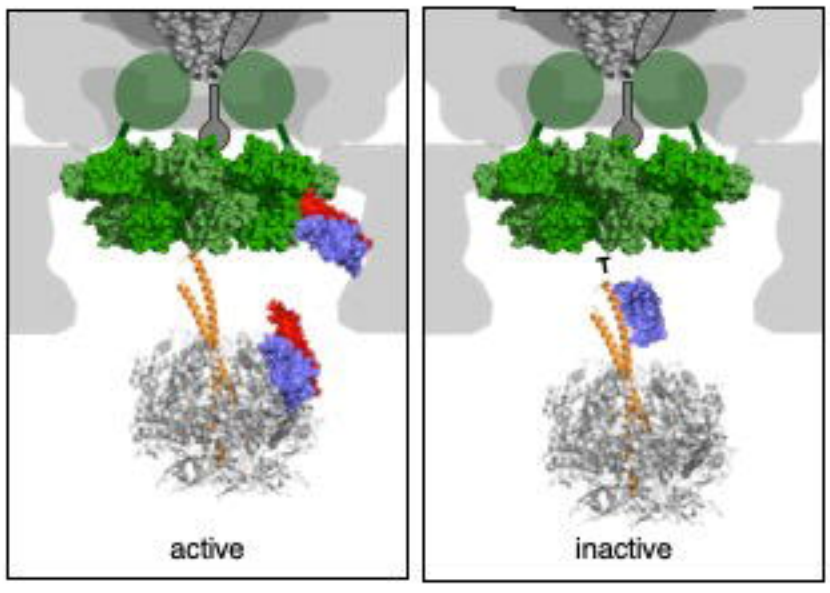
FIGURE 5